Nuclear Instruments and Methods in Physics Research A 719 (2013) 44–49

Contents lists available at SciVerse ScienceDirect

Nuclear Instruments and Methods in Physics Research A

journal homepage: www.elsevier.com/locate/nima

A superconducting magnet mandrel with minimum symmetry laminations for proton therapy

S. Caspi [a], D. Arbelaez [a], L. Brouwer [a,b,*], D.R. Dietderich [a], H. Felice [a], R. Hafalia [a], S. Prestemon [a], D. Robin [a], C. Sun [a], W. Wan [a]

[a] Lawrence Berkeley National Laboratory, 1 Cyclotron Road, Berkeley, CA 94720, USA
[b] University of California, Berkeley, 2200 University Drive, Berkeley, CA 94720, USA

ARTICLE INFO

Article history:
Received 4 December 2012
Received in revised form
6 March 2013
Accepted 4 April 2013
Available online 18 April 2013

Keywords:
Curved dipole magnet
Superconducting
Gantry
Hadron therapy
Canted cosine-theta

ABSTRACT

The size and weight of ion-beam cancer therapy gantries are frequently determined by a large aperture, curved, ninety degree, dipole magnet. The higher fields achievable with superconducting technology promise to greatly reduce the size and weight of this magnet and therefore also the gantry as a whole. This paper reports advances in the design of winding mandrels for curved, canted cosine-theta (CCT) magnets in the context of a preliminary magnet design for a proton gantry. The winding mandrel is integral to the CCT design and significantly affects the construction cost, stress management, winding feasibility, eddy current power losses, and field quality of the magnet. A laminated mandrel design using a minimum symmetry in the winding path is introduced and its feasibility demonstrated by a rapid prototype model. Piecewise construction of the mandrel using this laminated approach allows for increased manufacturing techniques and material choices. Sectioning the mandrel also reduces eddy currents produced during field changes accommodating the scan of beam energies during treatment. This symmetry concept can also greatly reduce the computational resources needed for 3D finite element calculations. It is shown that the small region of symmetry forming the laminations combined with periodic boundary conditions can model the entire magnet geometry disregarding the ends.

1. Introduction

State-of-the-art ion beam cancer therapy requires rotatable accelerator beamlines, called gantries, that direct and scan an ion beam over tumors from multiple angles [1–3]. This minimizes the dose delivered to surrounding healthy tissue. The size and weight of such gantries are primarily determined by their magnets. The most advanced scanning gantries (at the Heidelberg Ion Therapy Center and Gantry 2 at PSI) are Pavlovic style. For these designs a final, resistive, ninety degree, bending magnet required by the Pavlovic beam optics layout dominates these effects. Reducing the size and weight of this magnet and thus the gantry as a whole motivates the design of a high-field, superconducting, bending magnet.

In this paper we describe advancements in the design and analysis of winding mandrels for curved CCT gantry magnets. The mandrel is a critical component of the CCT design affecting the winding feasibility, cost, field quality, stress management, and eddy currents of the magnet. A laminated mandrel concept is presented in the context of a preliminary design of a ninety degree, superconducting, combined function, 3.5 T dipole magnet for use in a proton therapy gantry. The advantages of this concept for manufacturing the mandrel, addressing eddy currents during field changes, and simplifying numerical calculations are detailed.

In Section 2 we discuss the magnet requirements and the choice of the CCT style. Section 3 lists the magnet parameters and magnetic calculation results. Section 4 discusses tilted winding channels and the use of mandrel ribs to prevent Lorentz force accumulation. Section 5 describes a laminated mandrel concept and a rapid prototype model constructed to demonstrate this concept. Section 6 presents the necessary steps to complete the magnet design, including plans for further studies of the mechanical structure and cryogenic system.

2. Magnet requirements and choice of the CTT design

The final bending magnet in this type of particle therapy gantry has a unique combination of requirements. It must be large aperture, curved over a large angle, produce combined function

* Corresponding author at: 1 Cyclotron Road, M/S 46-161 Berkeley, CA 94720, USA. Tel.: +1 510 486 7244.
E-mail addresses: s_caspi@lbl.gov (S. Caspi), lnbrouwer@lbl.gov (L. Brouwer).

0168-9002/$ - see front matter © 2013 Elsevier B.V. All rights reserved.
http://dx.doi.org/10.1016/j.nima.2013.04.021

fields, and be capable of changing field quickly to accommodate beam energy variation (60–220 MeV for protons) during treatment scanning. Previous studies have shown adding a quadrupole and sextupole component to the dipole field is advantageous for focusing and minimizing beam distortion. They have also shown the capability of multilayer, canted coil designs to produce these multipoles within the bore of a torus [4]. The CCT design consists of layers oppositely tilted with respect to a bore axis (Fig. 2). The layers are powered so that within the bore the contributions of each layer to the solenoidal field cancel and the dipole field sum [8–14]. A specific conductor path generates a pure dipole field overlaid with quadrupole and sextupole terms. The desired combined function field can be created by optimizing this winding path.

The scale of the magnet design was chosen to suit treatment using protons up to 220 MeV in energy. The bore diameter, bending radius, and main dipole field are 130 mm, 634 mm, and 3.5 T respectively. A similar magnet for use with carbon ions would be about two times the size and have a 50% higher dipole field than this design [5–7]. The higher order multipole requirements are a quadrupole of −3.17 T/m and a sextupole of 1.84 T/m^2 (Figs. 1 and 2).

3. Magnet and field

Tables 1 and 2 summarize the magnet geometry and expected performance. The overall design approach depends strongly on the winding path and conductor size. We have elected to use an aluminum mandrel with machined channels to guide and retain a NbTi Rutherford cable (see Section 4). E2 fiberglass will be used for cable insulation and the coil will be impregnated. A preliminary coupling design between layers includes the impregnation of both layers to each other. A key and bladder assembly with an outer aluminum shell is being considered for the magnet structure. In this design the iron yoke is made of machined laminations roughly 20 mm in thickness that are tapered to match the curved geometry. The yoke is loaded by an aluminum shell (using keys and bladders) to oppose the operating radial Lorentz forces (Fig. 3). This method has been used in high field magnets to ensure sufficient pre-compression and minimize the possibility of conductor motion [15].

Magnetic analysis was done using Biot–Savart (no-iron) followed by 3D Tosca calculations including the contribution from real iron. Both models used a large number of elements for the coils in some cases resulting in run times up to a week in length. Fig. 1 shows a nominal dipole field of 3.5 T with a negative horizontal gradient and a positive sextupole superimposed on top of it (field calculations were done using Biot–Savart). The central dipole field on the mid-plane has a gradient of −3.17 T/m and a sextupole of 1.84 T/m^2. According to the load line (Fig. 4), the

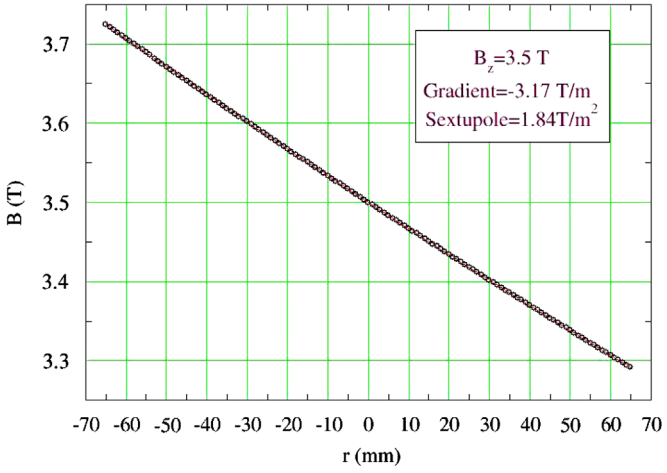

Fig. 1. Required field across the bore midplane.

Table 1
Magnet geometry.

Torus curvature radius	mm	634
Clear bore diameter	mm	130
Layer 1 inner diameter	mm	140
Layer to layer space	mm	5
Layer 2 outer diameter	mm	198.77
Bare cable width	mm	2.723
Bare cable thickness	mm	1.072
Cable insulation thickness	mm	0.150
Turns per channel	#	4
Iron inner diameter	mm	290
Iron outer diameter	mm	590
Aluminum shell thickness	mm	10

Table 2
Magnet parameters.

Strand diameter	mm	0.648
Strand type and Cu:Sc ratio	SSC outer	1.8:1
Number of strands per cable	#	8
Central dipole field/current at target	T/A	3.5/1320
Central dipole field/current at SS	T/A	5.25/2076
Conductor field/current at target	T/A	5.86/2076
Margin at target	%	67
Stored energy at target	kJ	134
Stored energy at SS	kJ	300
Aluminum shell stress at SS	MPa	220

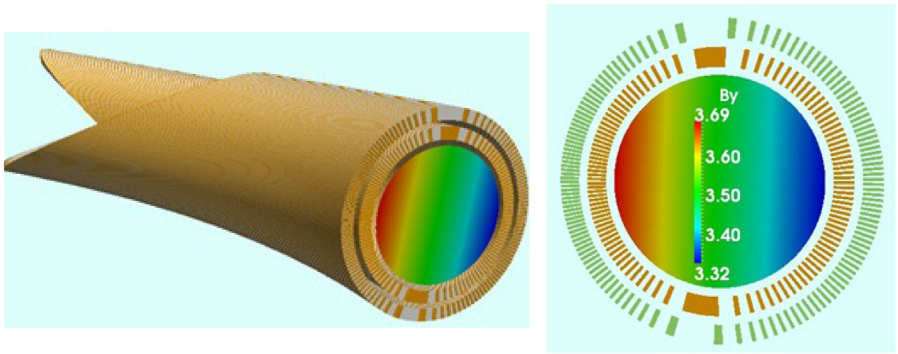

Fig. 2. Combined function fields inside the bore of a CCT toroidal magnet. The colors correspond to the magnitude of the dipole field (By).

magnet central field will reach 3.5 T at 1320 A having a 67% margin.

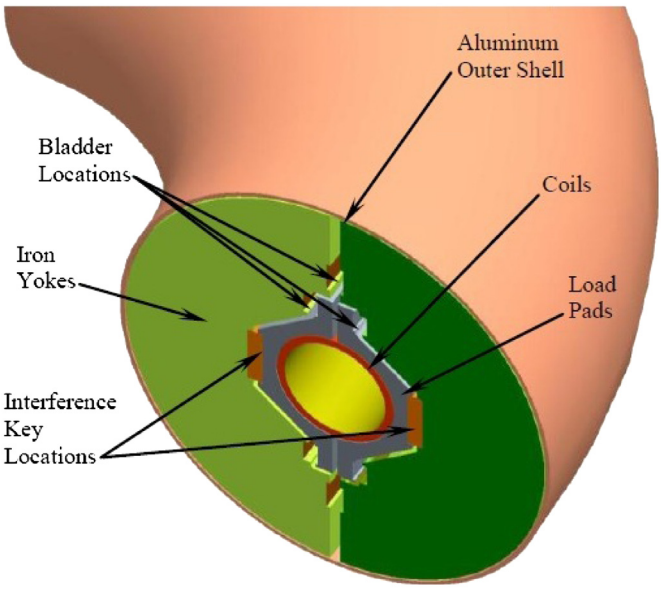

Fig. 3. Mechanical structure.

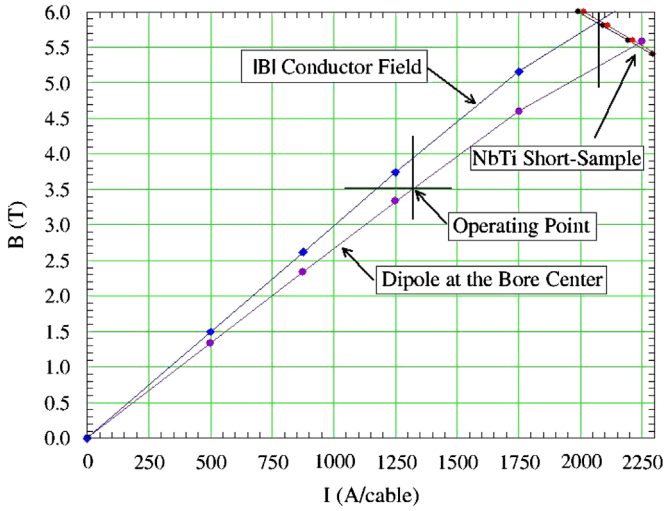

Fig. 4. Load line at the center of the bore and at the conductor.

4. Mandrel channel design and stress interception

In the CCT design each conductor layer requires its own winding mandrel. This mandrel is a curved tube with channels cut into it that guide the conductor around the bore (Fig. 6).

4.1. Windings and channel tilt

Rutherford cables made of twisted superconducting strands are typically used in superconducting accelerator magnets in part thanks to their flexibility when bent the "hard" way around magnet ends. Initially we decided to use a wide 23 strand cable. To reduce the effect of the hard bend on this cable the use of tilted channels, where the tilt orientation with respect to the bore varies azimuthally, was proposed. This allows the inner and outer edges of the cable to maintain a similar perimeter and reduce conductor strain.

A rapid prototype (RP) mandrel piece was created and this wide 23 strand cable was wound into its channels (requiring channel tilt). However, the difficulty experienced with this led to the wide cable approach being replaced by a stack of four smaller cables each made from eight strands. The smaller cable choice does not require tilted channels (they remain normal to the surface) to reduce conductor strain. The width of RP channel was designed as 12.09 mm to accommodate these four small sized cables wound on top of each other "edge to edge". The experience winding and stacking these four small sized cables into a rapid prototype model has proven to be much easier than winding the single wide conductor, even without the special consideration of a constant perimeter winding (Fig. 5).

4.2. Interception of stresses

A natural feature of this mandrel design is a variation in the channel wall thickness as the channel moves from the mid-plane

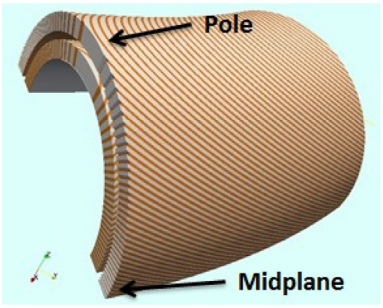

Fig. 6. View of the channels and conductor path.

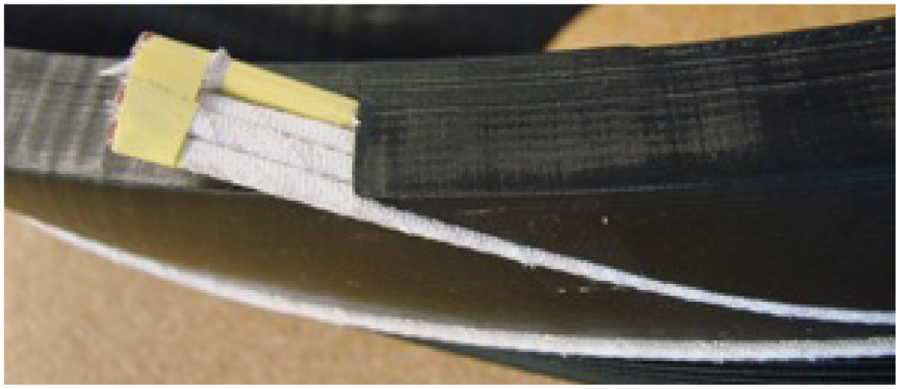

Fig. 5. Four nested cables wound into a single channel (RP model).

to the pole (Fig. 6). They are thin along the mid-planes, 1.1 mm and 0.7 mm on the torus outer and inner radii respectively, and thick at the poles (3.9 mm). We plan to use the channel walls (ribs) as intercepts to the Lorentz forces to prevent stress accumulation between turns. Incorporating the ribs as structural elements will require they are sufficiently thick to carry the load and prevent them from excessive bending. The intercepted Lorentz forces captured by the ribs will be guided towards the inner structural tubing to which the ribs are attached. The concept of intercepting Lorentz forces, also termed "stress-management", has been considered in the past for high field magnets [16]. Although the field here is relatively low, the concept of stress interception is also important due to the large bore and the large number of turns.

Using the Lorentz force (per unit length) we have estimated the operating applied stress both normal and radial to the channel (Fig. 7). The Lorentz force normal to the channel walls varies between the mid-plane and the pole in a "sine-theta" like manner (Fig. 7). This generates local stress close to zero near the mid-plane and up to 2.5 MPa at the pole. Note a beneficial feature of the CCT design is that the rib thickness varies similarly to the magnitude of the stress it intercepts. The radial stress on the cable varies azimuthal in a "cosine-theta" like manner, with 17 MPa near the mid-plane and zero near the poles.

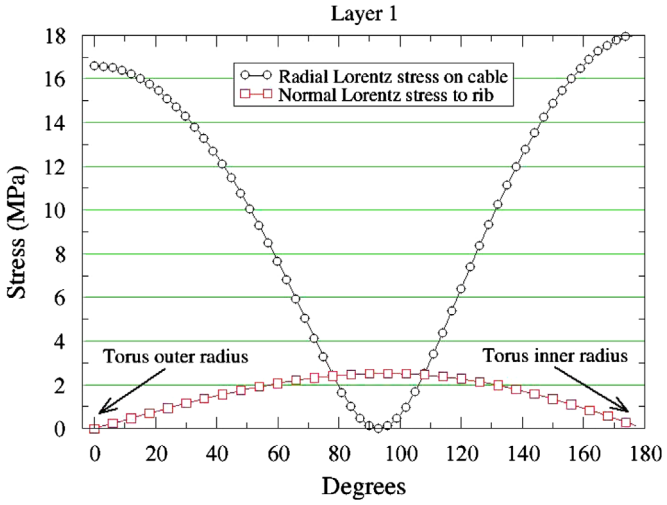

Fig. 7. The two orthogonal stress components generated across a single turn. The pole is located near 90° and the midplane at 0° and 180°.

5. A laminated mandrel design

A minimum symmetry in the CCT winding path allows for the entire mandrel to be made out of laminations stacked around the bend of the torus. For this design identical tapered laminations with thickness of a "pitch" ($\phi = 0.5^\circ$ where ϕ is the angle around the torus) repeat to form the mandrel (Fig. 8). Just like in a solenoid where the conductor size determines the turn to turn pitch, the conductor and rib sizes in the CCT in combination with the tilt angle determine the lamination and pitch length. Three important benefits of this laminated approach are increased manufacturing options, a reduction in eddy current power losses, and a simplification of numerical calculations.

5.1. Manufacturing

The minimum symmetry allows for the mandrel to be built piecewise out of small sections. This has the potential to simplify the production of the mandrel for cases where small identical laminations are easier to fabricate than machining channels into a single large piece. This size difference may allow for more advantageous manufacturing techniques and mandrel materials to be used.

5.2. Reduction in eddy current losses

Constructing the mandrel out of small laminations (that can be electrically isolated) reduces eddy currents produced within the mandrel as the magnet ramps to follow quick beam energy changes during treatment. The potential of thin laminations to reduce power loss is demonstrated by a similarly sized slab in a perpendicular time varying field. The eddy current power loss per volume within the top or bottom face of a long (non-laminated) rectangular tube is estimated by

$$\frac{P}{vol} = \frac{1}{12}\frac{d^2}{\rho}\dot{B}_z^{\,2}, \tag{1}$$

Table 3
Eddy current losses in a rectangular mandrel.

Property	Single piece	Laminated
Sections	1	180
Section length	1.0 m	5.56 mm
Mandrel width	136 mm	136 mm
Resistivity (aluminum at 4.2 K)	3.0×10^{-8} Ω m	3.0×10^{-8} Ω m
Total loss at $\dot{B} = 0.06$ T/s	1.5×10^{-1} W	2.5×10^{-4}
Total loss at $\dot{B} = 0.5$ T/s	10 W	1.7×10^{-2}

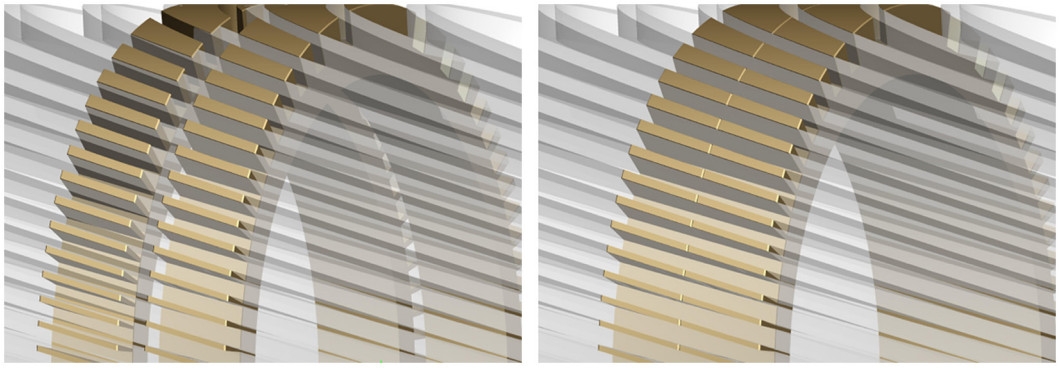

Fig. 8. Two adjacent mandrel laminations are shown (with a displacement in the left-hand image and mated on the right). These laminations are identical and the conductor channels match perfectly end to end, representing the periodic symmetry in the winding path.

where d is the length of the mandrel across the bore and perpendicular to the field. Assuming the lamination thickness l is much smaller than d, the power loss for a laminated mandrel scales by the lamination length l rather than d. This reduces the total losses by a factor of d^2/l^2. Using minimum symmetry laminations for a rectangular mandrel of similar size to layer one of the gantry magnet reduces the eddy current loses by an approximate factor of 600 (see Table 3).

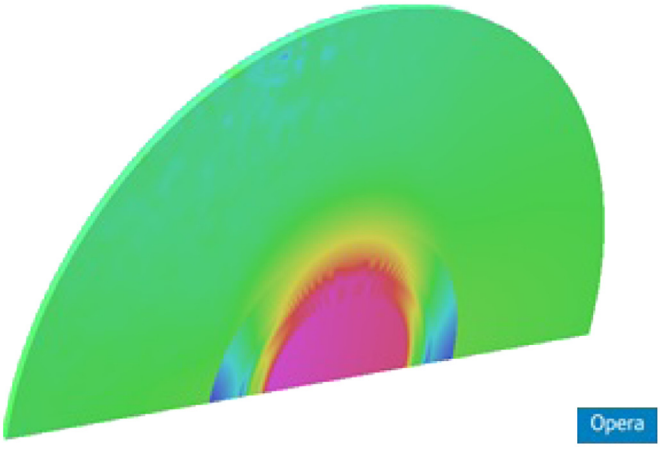

Fig. 9. View of the field (Bmod) across a single lamination (TOSCA model).

5.3. Simplification of finite element calculations

The minimum symmetry can also be used to simplify magnetic and structural finite element calculations. The small region of a single lamination can model the entire geometry of the magnet (excluding the ends) with the appropriate boundary conditions. In this magnet design a 3D calculation performed on a single section of symmetry requires only 1/180 of the total magnet volume. We have used the program Tosca to validate this by comparing a magnetic calculation using the entire magnet geometry to one performed on the lamination (Fig. 9). The periodic boundary condition used in this solution was applied by enforcing a magnetic potential equality constraint for matching nodes on opposite faces of the lamination.

5.4. A full scale rapid prototype

Short of making real parts, the use of a rapid-prototyping (RP) machine to produce plastic pieces has proven to be both time and cost effective. Small pieces were first used to test the effect of cable size on winding feasibility (Section 4.1). After the choice of cable and mandrel design was completed, a full size RP mandrel model was built (Figs. 10 and 11). This has a bending radius of 634 mm and clear bore of 130 mm. Due to the machine size limitations, the mandrel model had to be sectioned and then assembled after manufacturing. One of these sections was constructed out of 56 single laminations, demonstrating the laminated concept (red portion in Fig. 10). After being assembled the mandrel was successfully wound with a single layer of eight strand superconducting cable.

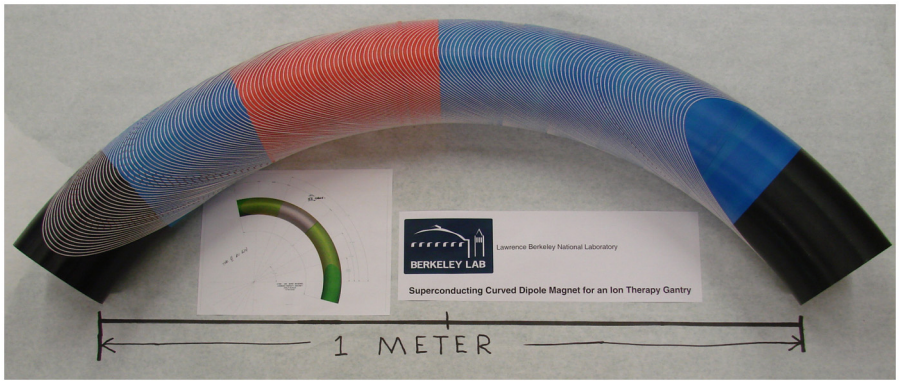

Fig. 10. A full size 90° rapid prototype mandrel is shown wound with eight strand superconducting cable. The red section was created from stacked laminations (See Fig. 11). (For interpretation of the references to color in this figure caption, the reader is referred to the web version of this article.)

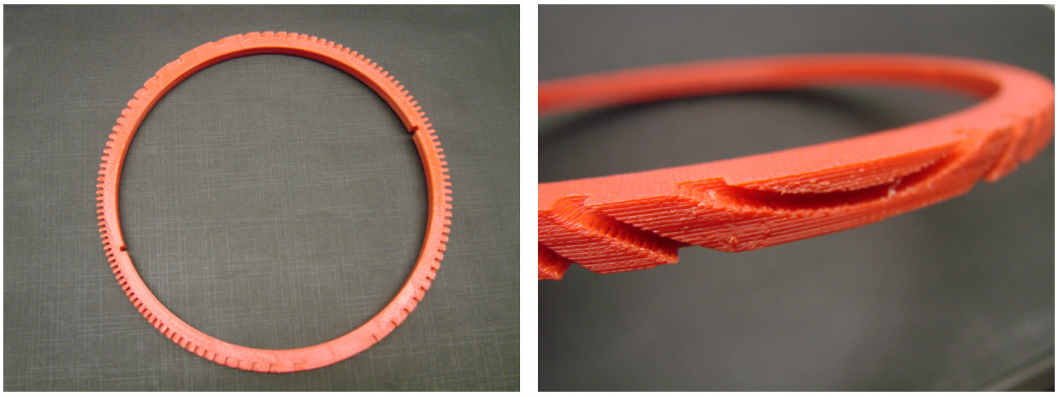

Fig. 11. A single lamination piece made using a rapid prototype machine.

6. Future plans

The next steps in the development of a curved gantry dipole magnet will be focused on a detailed stress analysis (during assembly, cool down, and operation), the interaction between coils, mandrel, structure, and the construction of the magnet. This leads to a complete lamination and layer-to-layer connection scheme as well as an overall understanding of the fine coupling between mechanical parts in the curved structure. Cryogenic options must also be examined with consideration given to rotation during operation. Similar steps are being taken in our high field magnet program for a straight bore CCT magnet. We have started the design, analysis, and construction of a sub-scale 4 T magnet to study the performance and field quality of the CCT design.

Acknowledgments

This work was supported by the Director, Office of Science, Office of Energy Research, Office of High Energy and Nuclear Physics, High Energy Physics Division, US Department of Energy, under Contract no. DE-AC02-05CH11231, and the National Science Foundation under Grant no. DGE 1106400. The authors greatly appreciate the interest and enthusiastic support of Andrew Sessler and are thankful for funding received within our laboratory through LDRD.

References

[1] M. Pavlovic, E. Griesmayer, R. Seemann, Nuclear Instruments and Methods in Physics Research Section A 545 (2005) 412.
[2] U. Weinrich, in: Proceedings of the 2006 European Particle Accelerator Conference, Edinburgh, Scotland, 2006, pp. 964–968.
[3] R. Fuchs, et al., in: Proceedings of the 2004 EPAC Conference, 2004, pp. 2550–2552.
[4] D.S. Robin, D. Arbelaez, S. Caspi, A. Sessler, C. Sun, W. Wan, M. Yoon, Nuclear Instruments and Methods in Physics Research Section A 659 (2011) 484.
[5] S. Caspi, D. Arbelaez, H. Felice, R. Hafalia, D. Robin, C. Sun, W. Wan, M. Yoon, IEEE Transactions on Applied Superconductivity 22 (3) (2012) 4401204.
[6] C. Sun, D. Arbelaez, S. Caspi, D. Robin, A. Sessler, W. Wan, M. Yoon, Compact beam delivery system for ion beam therapy, in: Proceedings of the IPAC2011, San Sebastian, Spain, 2011, pp. 3633–3635.
[7] S. Caspi, D. Arbelaez, L. Brouwer, D. Dietderich, R. Hafalia, D. Robin, A. Sessler, C. Sun, W. Wan, Progress in the design of a curve superconducting dipole for a therapy gantry, in: Proceedings of the IPAC2012, New Orleans, Louisiana, 2012, pp. 4097–4099.
[8] D.I. Meyer, R. Flasck, Nuclear Instruments and Methods in Physics Research Section A (1970) 339.
[9] C.L. Goodzeit, M.J. Ball, R.B. Meinke, IEEE Transactions on Applied Superconductivity 13 (June (2)) (2003) 1365.
[10] A.V. Gavrilin, et al., IEEE Transactions on Applied Superconductivity 13 (June (2)) (2003) 1213.
[11] A. Devred, et al., Superconductor Science and Technology 19 (2006) 67.
[12] C. Goodzeit, R. Meinke, M. Ball, Combined function magnets using double-helix coils, in: Proceedings of the Particle Accelerator Conference, 2007 PAC IEEE, 2007, pp. 560–562.
[13] S. Caspi, D.R. Dietderich, P. Ferracin, N.R. Finney, M.J. Fuery, S.A. Gourlay, A. R. Hafalia, IEEE Transactions on Applied Superconductivity 17 (part 2) (2007) 2266.
[14] H. Witte, T. Yokoi, S.L. Sheehy, K. Peach, S. Pattalwar, T. Jones, J. Strachan, N. Bliss, IEEE Transactions on Applied Superconductivity 2 (2012) 4100.
[15] S. Caspi, S. Gourlay, R. Hafalia, A. Lietzke, J. O'Neill, C. Taylor, A. Jackson, IEEE Transactions on Applied Superconductivity 11 (1) (2001) 2272.
[16] A. McInturff, et al., IEEE Transactions on Applied Superconductivity 17 (2) (2007) 1157.